OBSERVER BASED ROBUST CONTROL

S J Dodds
School of Computing and Technology, Control Research Group
stephen.dodds@spacecon.co.uk; s.j.dodds@uel.ac.uk

Abstract: This paper presents an original contribution to the field of robust control. Plant order uncertainty as well as parametric uncertainty is catered for while guaranteeing not only closed loop stability but also a precisely prescribed closed loop dynamic response to the reference inputs. The method extends to nonlinear multivariable plants. Its ability to control plants having different orders *without adjustment and yielding the same closed-loop dynamics* is demonstrated by simulation of its application to speed control and position control of a permanent magnet synchronous motor drive. The model of the plant used in the observer can simply be a chain of integrators driven by each control variable, at least equal in number to the rank of the plant with respect to the associated controlled output. The controller is simple, requires no adjustment and requires little more computational power than a typical classical PID controller.

1. Introduction

Observer based robust control (OBRC) is a new control technique, applicable to linear or nonlinear uncertain plants subject to unknown disturbances, that achieves robustness according to the following definition:

> *The robustness of a control system is defined as its ability to produce a specified closed loop dynamic response to reference inputs, within acceptable error tolerances for the application in hand, despite a) uncertainties in the assumed plant model used for the control system design and b) unknown external disturbances.*

By a specified closed loop dynamic response is meant the output response to a given reference input determined by a specified differential equation. The error tolerances are included to allow acceptably small departures from the ideal closed-loop response.

By an 'uncertain plant' is meant a plant whose mathematical model is not known accurately: In addition to lack of accurate knowledge of the plant parameters, the uncertainty may also be in the plant order.

OBRC superficially resembles internal model control (IMC) developed principally for the process control industry and later modified to cater for unstable plants (Yamada, 1999). There may be theoretical links between them, but the underlying strategies are different, IMC being formulated using transfer functions and therefore restricted to linear plants, while OBRC is formulated in the time domain and extends to nonlinear, multivariable plants. Also the block diagram structures presented in this paper are different from those of IMC.

The underlying concept of OBRC will now be introduced, commencing with the 'plant model mismatch equivalent input' premise upon which the method is based and followed by the formation of the controller using this special input. The introduction of an observer to render the method practicable by estimation of the plant model mismatch equivalent input will then be presented. Then some illustrative examples will be given.

2. Underlying Concepts

2.1. Plant model mismatch equivalent input.

The applicability of the OBRC method depends on the existence of a *plant model mismatch equivalent input,* $\mathbf{u}_e$, the meaning of which is defined in Fig. 2.1.

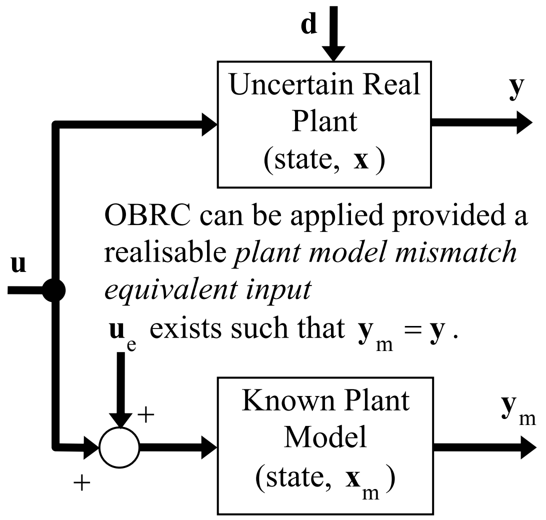

Fig. 2.1: Plant model mismatch equivalent input.

2.2. Theory of OBRC.

Consider a plant described by a state space model of the following general form:

$$\begin{cases} \dot{\mathbf{x}} = \mathbf{F}(\mathbf{x},\mathbf{u},\mathbf{d}) \\ \mathbf{y} = \mathbf{H}(\mathbf{x}) \end{cases} \tag{2.1}$$

where $\mathbf{x} \in \Re^n$ is the state vector, $\mathbf{u} \in \Re^r$ is the control vector, $\mathbf{d} \in \Re^q$ is the vector of all disturbances acting at various points in the plant and $\mathbf{y} \in \Re^m$ is the vector of measurements, assumed here to be also the vector of controlled variables. $\mathbf{F}(\bullet)$ and $\mathbf{H}(\bullet)$ are continuous functions of their arguments. Also $\mathbf{H}(\mathbf{0}) = \mathbf{0}$. A necessary condition for controllability, in the sense of being able to independently control each of the measurement variables, is $r \geq m$.

Now let a model of the plant (2.1) be created:

$$\begin{cases} \dot{\mathbf{x}}_m = \mathbf{F}_m(\mathbf{x}_m,\mathbf{u}_m) \\ \mathbf{y}_m = \mathbf{H}_m(\mathbf{x}_m) \end{cases} \tag{2.2}$$

where $\mathbf{x}_m \in \Re^N$, $\mathbf{u}_m \in \Re^r$ and $\mathbf{y}_m \in \Re^m$. As for the real plant, $\mathbf{F}_m(\bullet)$ and $\mathbf{H}_m(\bullet)$ are continuous functions of their arguments and $\mathbf{H}_m(\mathbf{0}) = \mathbf{0}$. The model is mismatched with respect to the real plant in three respects:

a) it does not have a disturbance input,
b) its parameters may differ from the real plant parameters and furthermore,
c) model order uncertainty is included by allowing $N \neq n$ but, as will be seen, there will be a restriction regarding the relative degrees of the plant with respect to each controlled output.

It is reasonable to assume that $\mathbf{u}_m$ and $\mathbf{u}$ have the same dimensions and also that $\mathbf{y}_m$ and $\mathbf{y}$ have the same dimensions. Now suppose that the real plant (2.1) and its model (2.2) are fed by the same arbitrary control vector, $\mathbf{u}_m(t) = \mathbf{u}(t)$, with zero initial states, $\mathbf{x}_m(0) = \mathbf{0}$ and $\mathbf{x}(0) = \mathbf{0}$. Then $\mathbf{y}_m(0) = \mathbf{y}(0) = \mathbf{0}$, but in view of (a),

(b) and (c) above, $\mathbf{y}_m(t) \neq \mathbf{y}(t)$ for $t > 0$. Now the whole theory rests on the existence of a *plant model mismatch equivalent input*, $\mathbf{u}_e(t)$, such that if $\mathbf{u}_m(t) = \mathbf{u}(t) + \mathbf{u}_e(t)$, then $\mathbf{y}_m(t) = \mathbf{y}(t)$ $\forall t > 0$. Thus:

$$\begin{cases} \dot{\mathbf{x}}(t) = \mathbf{F}(\mathbf{x}(t), \mathbf{u}(t), \mathbf{d}(t)) \\ \dot{\mathbf{x}}_m(t) = \mathbf{F}_m(\mathbf{x}_m(t), \mathbf{u}(t) + \mathbf{u}_e(t)) \\ \mathbf{y}(t) = \mathbf{y}_m(t) = \mathbf{H}(\mathbf{x}(t)) = \mathbf{H}_m(\mathbf{x}_m(t)) \end{cases} \quad (2.3)$$

Differentiating the last of equations (2.3) with respect to time:

$$\dot{\mathbf{y}}(t) = \dot{\mathbf{y}}_m(t) = \frac{\partial \mathbf{H}(\mathbf{x})}{\partial \mathbf{x}}.\dot{\mathbf{x}} = \frac{\partial \mathbf{H}_m(\mathbf{x}_m)}{\partial \mathbf{x}_m}.\dot{\mathbf{x}}_m \quad (2.4)$$

where the Jacobean matrices are defined in usual way. Substituting for $\dot{\mathbf{x}}$ and $\dot{\mathbf{x}}_m$ in (2.4) using the first two equations of (2.3) then yields:

$$\frac{\partial \mathbf{H}(\mathbf{x})}{\partial \mathbf{x}}.\mathbf{F}(\mathbf{x}, \mathbf{u}, \mathbf{d}) = \frac{\partial \mathbf{H}_m(\mathbf{x}_m)}{\partial \mathbf{x}_m}.\mathbf{F}_m(\mathbf{x}_m, \mathbf{u} + \mathbf{u}_e) \quad (2.5)$$

The application of OBRC therefore depends on the existence of a finite solution of (2.5) for $\mathbf{u}_e$, and this can be used as a theoretical tool to determine whether or not OBRC can be applied in particular cases, prior to attempting a control system design. If (2.5) is soluble, then if $\mathbf{u}_e$ were to be known, it would be possible to form a primary control vector, $\mathbf{u}'$, such that

$$\mathbf{u} = \mathbf{u}' - \mathbf{u}_e \quad (2.6)$$

Substituting this into (2.1) and (2.2) then yields:

$$\dot{\mathbf{x}}(t) = \mathbf{F}(\mathbf{x}, \mathbf{u}' - \mathbf{u}_e, \mathbf{d}) \quad (2.7)$$

$$\dot{\mathbf{x}}_m = \mathbf{F}_m(\mathbf{x}_m, \mathbf{u}'), \ \mathbf{y} = \mathbf{y}_m \quad (2.8)$$

Equations (2.8) has proven that the problem has been reduced to that of controlling the known model with the primary control vector, $\mathbf{u}'$. All that remains is to find a means of accurately estimating $\mathbf{u}_e$. This can be done quite simply by applying an observer to plant (2.1) with its real time model given by (2.2), as depicted in Fig. 2.2. By comparison with Fig. 2.1, it is clear that if the observer correction loop is designed to drive the model output error, $\mathbf{e}_m$, to negligible proportions, then $\hat{\mathbf{u}}_e \cong \mathbf{u}_e$. This, however, entails employing relatively high gains and care must be taken not to introduce too much sensitivity to measurement noise.

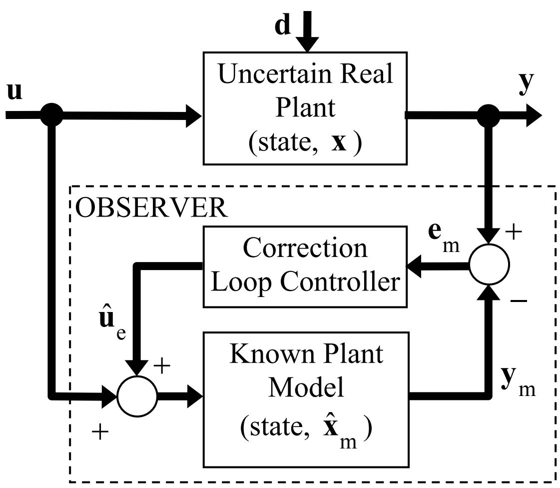

Fig. 2.2: Observer to estimate $\mathbf{u}_e$.

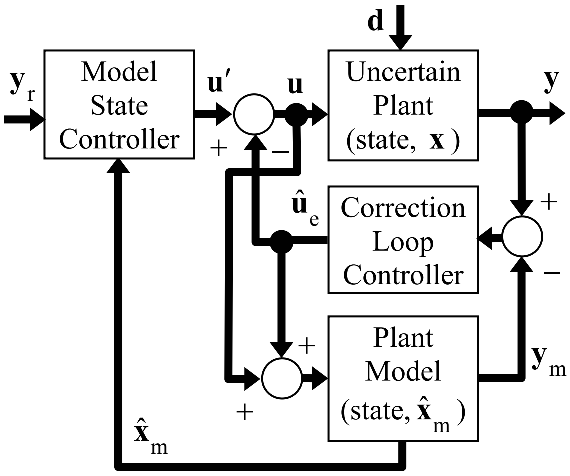

a) Subtraction of $\hat{\mathbf{u}}_e$ from plant and model inputs.

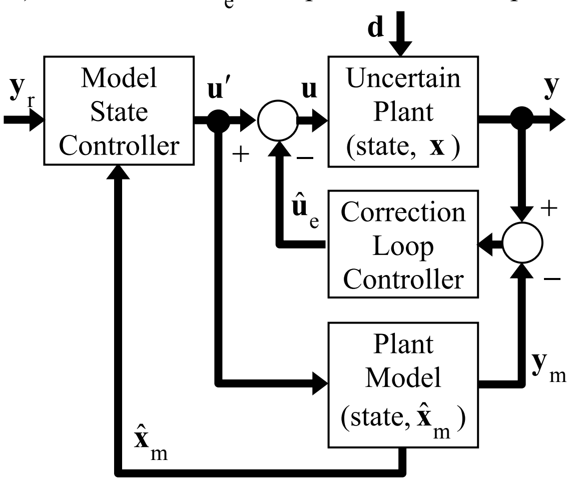

b) Simplification of input connections.

Fig. 2.3: Structure of OBRC.

Since the plant model must be mismatched with respect to the real plant, the well known separation theorem of control system design doesn't strictly apply and to prove closed loop stability, the system as a whole would have to be analysed. Intuitively, however, the measurement vector, $\mathbf{y}$, can be regarded as a disturbance input to the observer correction loop that is 'rejected' by being counteracted by $\mathbf{y}_m$ if the correction loop gains are sufficiently high and determined using only the plant model. This has been confirmed by many simulations and some experiments currently under way but further theoretical work is needed from an academic viewpoint.

The control system is completed by forming the primary control input according to (2.6), followed by loop closure around the model using a state feedback controller to generate the primary control input, as shown in Fig. 2.3 (a). After simplification of the input connections, Fig. 2.3 (b) shows that the subtraction of $\hat{\mathbf{u}}_e$ from the plant and model causes only $\mathbf{u}'$ to be applied to the plant model and the correction loop controller to be applied to the plant. Remarkably, this proves to be a method of applying a high gain loop to an *unknown* plant while ensuring stability.

2.3. Choice of observer plant model.

In cases where a linear plant model is readily available, then it is recommended that this is used as a basis for the controller design. If not, however, modelling can be the most time consuming and therefore costly activity required to produce a control system design. OBRC can avoid this and provide robustness since, remarkably, there is no requirement for the plant model to closely resemble the real plant for equation (2.5) to be readily soluble. With this freedom, the plant model is chosen as *chains of integrators* separately driven by each control input. Not only will this yield straightforward design of the two controllers in Fig. 2.3 but for multivariable plants, ensure elimination of closed loop interaction between control channels. The observer then comprises r separate single input, single output sub-observers as shown in Fig. 2.4.

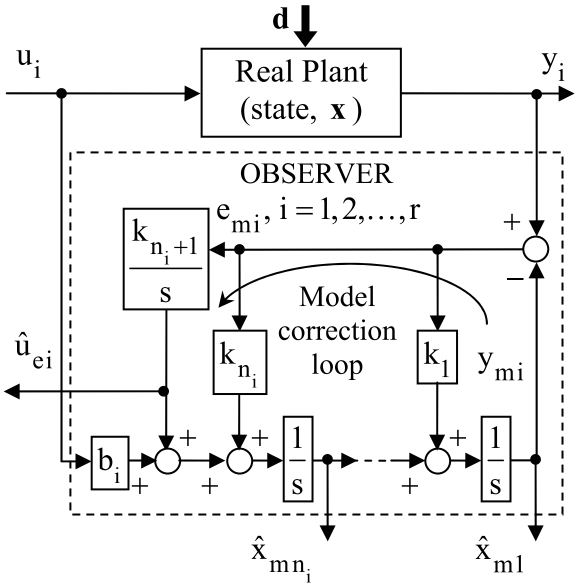

Fig. 2.4: Multiple integrator based observer.

Although it would make no difference to the response of the ideal system in which $e_{mi} = 0$ the integrator chain gain, b_i, is included as an adjustable parameter because with finite observer gains it would affect the accuracy of $\hat{u}_{ei}$.

Finally but importantly, if the total number of integrators in the chains is less than the plant order and the plant is of full rank, i.e., the sums of the relative degrees with respect to each output is equal to the plant order, then the order of the closed-loop system would be less than the plant order, resulting in closed-loop modes, unobservable by viewing the reference inputs and outputs, that could be *unstable*. This could be avoided by making the total number of integrators exceed the plant order but for plants not of full rank, there would be zero dynamics of the closed loop system unobservable in the aforementioned sense similar to that experienced in sliding mode control (Utkin, 1992). This would also enable the controller to accommodate a range of plants of different orders in a similar fashion to hyper-sliding mode control (Dodds, 2006) *while yielding the same closed loop dynamics*.

A method commonly included in state controllers for electric drives (Vittek and Dodds, 2003) to estimate external disturbances is to add an integrator to the observer model, as exemplified by the additional integrator with gain, k_{n_i+1}, in Fig. 2.4. In view of the OBRC theory presented in section 2.2, this also includes the effects of the mismatched between the plant and its model so the output of this integrator can be taken as $\hat{u}_{ei}$. Inclusion of this integrator also ensures zero steady-state error between $\mathbf{y}_r$ and $\mathbf{y}$ due to constant components of $\mathbf{d}$. The model correction loop of Fig. 2.4, however, is not of the same form as that of Fig. 2.2, several different correction paths being implemented instead of one. Fig 2.4, however, could be converted to the same form with a single correction loop controller. This would entail adding derivative terms to the 'k_{n_i+1}' integrator output but since the observer of Fig. 2.4 is sufficient to estimate $\mathbf{u}_e$, using the precise observer structure of Fig. 2.2 will be left to a future investigation.

3. Speed and position control of a synchronous motor drive.

3.1 Modelling and OBRC formulation.

The permanent magnet synchronous motor (PMSM) is modelled in the synchronously rotating d-q co-ordinate system by the following set of state differential equations:

$$di_d/dt = -Ai_d + B\omega_r i_q + Fu_d \quad (3.1)$$

$$di_q/dt = -C\omega_r i_d - Di_q - E\omega_r + Gu_q \quad (3.2)$$

$$d\omega_r/dt = \left(H + Ki_d\right)i_q - M\Gamma_L \qquad (3.3)$$

$$d\vartheta_r/dt = \omega_r \qquad (3.4)$$

where i_d, i_q and u_d, u_q are the stator current and voltage components, ω_r is the rotor angular velocity and Γ_L is the external load torque (Vittek & Dodds, 2003). Here:

$$\begin{cases} A = R_s/L_d; & F = 1/L_d \\ B = pL_q/L_d; & G = 1/L_q \\ C = pL_d/L_q; & H = 3p\Psi_{PM}/(2J_r) \\ D = R_s/L_q; & K = 3p(L_d - L_q)/(2J_r) \\ E = p\Psi_{PM}/L_q; & M = 1/(J_r + J_L) \end{cases}$$

Ψ_{PM} is the permanent magnet flux, R_s is the stator resistance, L_d and L_q are the direct and quadrature axis inductances, J_r and J_L are the rotor and load moments of inertia and p is the number of pole pairs. For position and speed control, the controlled measurement variables will be, respectively:

$$y_1 = \vartheta_r \quad (3.5) \qquad y_2 = \omega_r \quad (3.6)$$

These measurements are derived from shaft encoder outputs and are scaled to be numerically equal to the physical quantities being measured. There will be an additional controlled measurement variable:

$$y_3 = K_I i_d \qquad (3.7)$$

since this has to be controlled with $y_{3r} = 0$ to maintain the flux and current vectors mutually perpendicular for maximum torque generation efficiency (vector control). It is clear from (3.1) and (3.7) that the relative degree is 1 w.r.t. y_3, because the control variable, u_d, already appears on the RHS of (3.1), so only one integrator is required in the lower integrator chain of Fig. 2.4. For the speed control, differentiating (3.6) twice and substituting for di_q/dt using (3.2) yields the other control variable, u_q, on the right hand side and therefore the rank is 2 w.r.t. y_2. It is 3 w.r.t. y_1 due to the kinematic integrator in (3.4) and this would require three integrators in the lower chain of Fig. 2.4. The same controller will be used for y_2 as the number of integrators in the chain exceeds the plant rank w.r.t. this output by 1, which is acceptable. Fig. 3.1 shows a block diagram of the complete observer based robust control system (switch S to y_2 or y_1). The subscripts, r and y, refer, respectively to reference inputs and measurements and the transformations are as follows, with intermediate stator-fixed α-β frame:

$$\begin{bmatrix} i_{dy} \\ i_{qy} \end{bmatrix} = \underbrace{\underbrace{\begin{bmatrix} \cos\theta & \sin\theta \\ -\sin\theta & \cos\theta \end{bmatrix}}_{\substack{\text{Park Transformation} \\ T_{\alpha\beta\to dq}}} \underbrace{\begin{bmatrix} \frac{2}{3} & -\frac{1}{3} & -\frac{1}{3} \\ 0 & \frac{1}{\sqrt{3}} & -\frac{1}{\sqrt{3}} \end{bmatrix}}_{\substack{\text{Clark transformation} \\ T_{abc\to\alpha\beta}}}}_{T_{abc\to dq}} \begin{bmatrix} i_{ay} \\ i_{by} \\ i_{cy} \end{bmatrix}, \quad y_3 = i_{dy} \qquad (3.8)$$

$$\begin{bmatrix} u_{ar} \\ u_{br} \\ u_{cr} \end{bmatrix} = \underbrace{\underbrace{\begin{bmatrix} 1 & 0 \\ -\frac{1}{2} & \frac{\sqrt{3}}{2} \\ -\frac{1}{2} & -\frac{\sqrt{3}}{2} \end{bmatrix}}_{\substack{\text{Inverse Clark} \\ \text{Transformation} \\ T_{\alpha\beta\to abc}}} \underbrace{\begin{bmatrix} \cos\theta & -\sin\theta \\ \sin\theta & \cos\theta \end{bmatrix}}_{\substack{\text{Inverse Park} \\ \text{Transformation} \\ T_{dq\to\alpha\beta}}}}_{T_{dq\to abc}} \begin{bmatrix} u_{dr} \\ u_{qr} \end{bmatrix} \qquad (3.9)$$

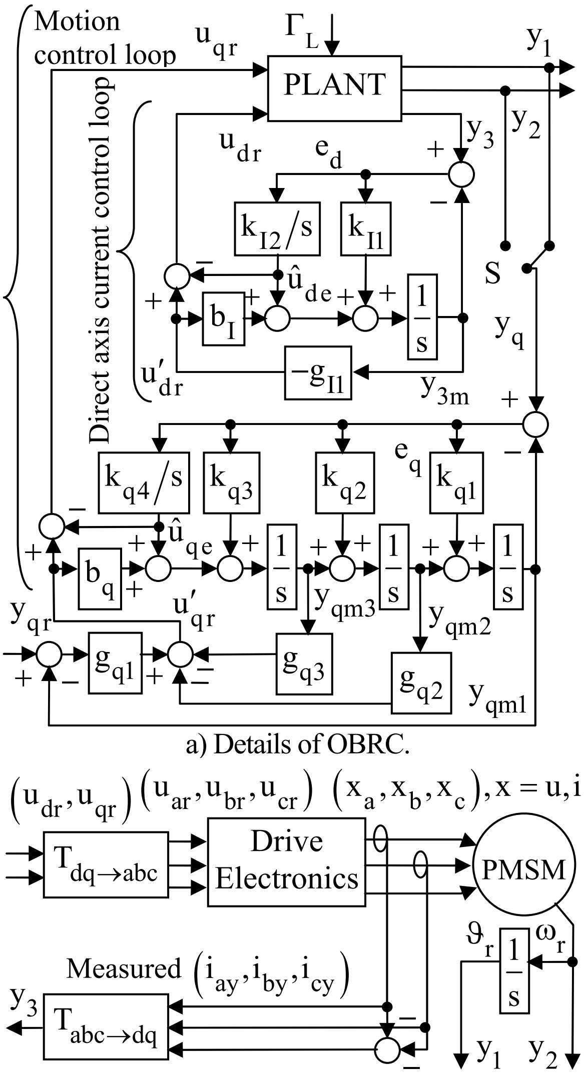

a) Details of OBRC.

b) Plant: drive electronics and measurement blocks, with 2/3 and 3/2 phase transformations.

Fig. 3.1: OBRC applied to electric drive for position or speed control.

Figure 3.2 shows a block diagram of the motor based on the two-phase model (3.1) to (3.4) with transformations (3.8) and (3.9) for the three-phase stator voltages and currents. Since the real time models are chosen as integrator chains, design by pole placement is very straightforward and mathematically similar for the observers and model state controllers. Applying the author's settling time formula (Vittek and Dodds, 2003) the characteristic polynomial for n coincident

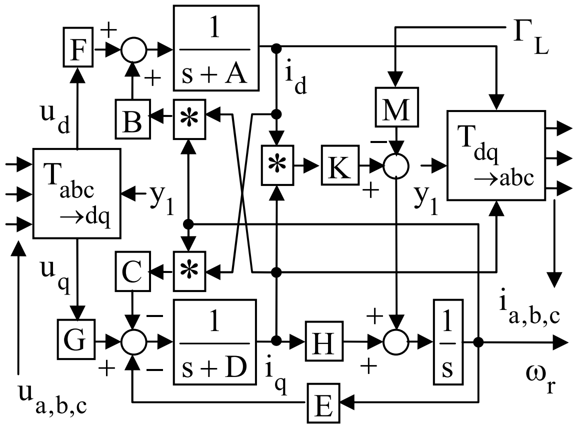

Fig. 3.2: Model of motor with transformations for three-phase stator voltages and currents.

poles and a settling time, T_s, is given by:

$$\left[s + 1.5(1+n)/T_s\right]^n \qquad (3.10)$$

Applying this with the appropriate values of n and the specified settling times, T_{soI}, T_{scI}, T_{soq} and T_{scq} of the observer correction loops and then equating with these characteristic polynomials obtained from Fig. 3.1 (a) using Mason's formula, yields:

$$s^2 + k_{I1}s + k_{I2} = s^2 + \frac{9}{T_{soI}}s + \frac{81}{4T_{soI}^2}$$

$$s^4 + k_{q1}s^3 + k_{q2}s^2 + k_{q3}s + k_{q4} = s^4 + \frac{4a}{T_{soq}}s^3 + \frac{6a^2}{T_{soq}^2}s^2 + \frac{4a^3}{T_{soq}^3}s + \frac{1}{T_{soq}^4}, \quad a = \frac{15}{2}$$

$$s + g_{I1} = s + 3/T_{scI}$$

$$s^3 + g_{q3}s^2 + g_{q2}s + g_{q1} = s^3 + \frac{18}{T_{scq}}s^2 + \frac{108}{T_{scq}^2}s + \frac{216}{T_{scq}^3}$$

Equating coefficients of like degree terms in s then yields to following gain equations:

$$k_{I1}=\frac{9}{T_{soI}},\ k_{I2}=\frac{81}{4T_{soI}^2},\ g_{I1}=\frac{3}{T_{scI}} \quad (3.11a)$$

$$\left.\begin{array}{l} k_{q1}=4a/T_{soq},k_{q2}=6a^2/T_{soq}^2 \\ k_{q3}=4a^3/T_{soq}^3,k_{q4}=a^4/T_{soq}^4 \end{array}\right\} a=\frac{15}{2} \quad (3.11b)$$

$$g_{q3}=\frac{18}{T_{scq}},\ g_{q2}=\frac{108}{T_{scq}^2},\ g_{q1}=\frac{216}{T_{scq}^3} \quad (3.11c)$$

3.2. Simulations

The PMSM parameters are as follows:

$J_r=0.003\ \text{Kgm}^2$; $p=3$; $L_d=1.4\ \text{H}$; $L_q=0.1618\ \text{H}$;

$R_s=36.5$; $\Psi_{PM}=0.312\ \text{Wb}$.

The mechanical load moment of inertia is $J_L=0.01\ \text{Kgm}^2$. The current transducer gain is $K_I=0.5\,\text{V/A}$. The position and velocity measurements are assumed to obtained from a shaft encoder and scaled to be numerically in rad/s and radians, so $K_\omega=K_\vartheta=1$.

The effects of a power electronic drive with a 300V d.c. link voltage with a switching frequency of 20 kHz is simulated by applying corresponding square wave perturbations to u_{ir} to obtain u_i, $i=a,b,c$.

The OBRC parameters are set to $T_{scI}=T_{scq}=0.2\,\text{s}$ and $T_{soI}=T_{soq}=0.05\,\text{s}$.

All the simulations start with zero initial conditions. For speed control, the step reference angular velocity is $y_{2r}=K_\omega\omega_{rr}$ where $\omega_{rr}=200\ \text{rad/s}$ and for position control, the step reference angle is $y_{1r}=K_\vartheta\vartheta_{rr}$ where $\vartheta_{rr}=2\ \text{rad}$. The robustness against external disturbances is assessed by applying an external load torque, $\Gamma_L(t)$, at $t=0.5\,\text{s}$ that ramps at $100\,\text{Nm/s}$ to a constant value of 3 Nm.

The integrator chain gains are $b_I=1$; $b_q=600$.

Fig. 3.3 and Fig. 3.4 show the speed and position control responses.

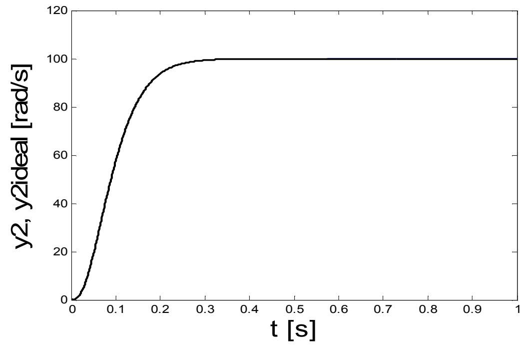

a) Rotor speed and ideal responses

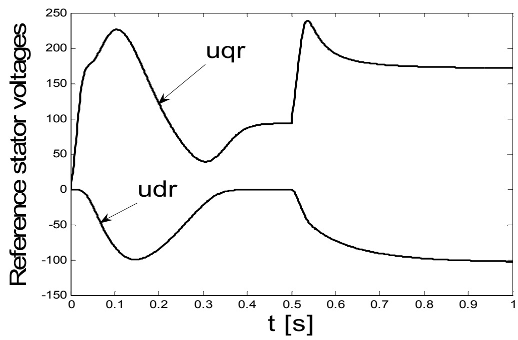

b) Control variables

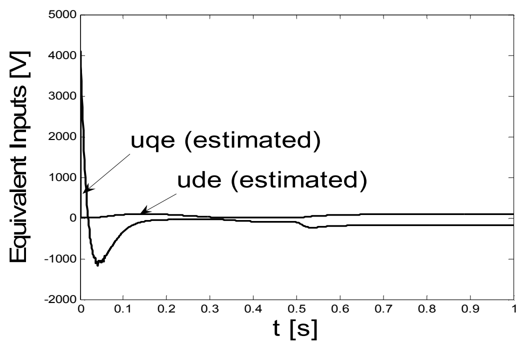

c) Model mismatch equivalent inputs.

Figure 3.3: Speed control.

4. Conclusions and recommendations

Despite the plants simulated being different, *even in order*, the response shapes are identical and indistinguishable from the ideal responses and the errors due to the load torque are invisible on the scales of the reference inputs. The control variables needed are, of course, very different. The model mismatch equivalent input for the q-axis exceeds the supply voltage but this is not problematic because it is only an internal

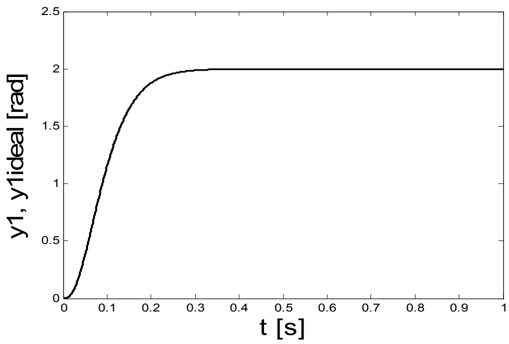

a) Rotor angle and ideal responses

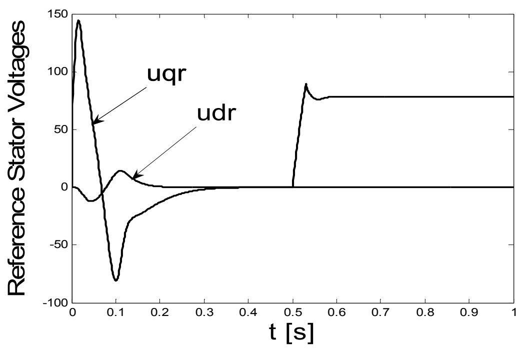

b) Control variables. Fig. 3.4: Position control.

variable in the control computer, the physical control inputs staying within a practicable limits of $\pm 400\,\mathrm{V}$.

OBRC is a promising new control method but theoretical work must be done regarding stability limits in view of the need to employ finite observer gains in practice.

5. References

Yamada, K., 'Modified Internal Model Control for Unstable Systems', *Proceedings of MED99,* Haifa, Israel, June 28-30, 1999.

Utkin, V. I., *Sliding Modes in Control and Optimisation*, Springer Verlag, 1992.

Dodds, S. J., "Hyper Sliding Mode Control", *Proceedings of AC&T 2006.*

J. Vittek and S. J. Dodds, *Forced Dynamic Control of Electric Drives*, Research Monograph, University of Zilina Press, 2003, ISBN 80-8070-087-7.